Characterization of Segregated Grout Promoting Corrosion of Posttensioning Tendons

Maddalena Carsana[1] and Luca Bertolini[2]

Abstract: Segregation of grout applied for the protection of posttensioning steel may cause corrosion of steel wires, leading to serious hazards to the safety of posttensioned structures. Several cases of failure of external tendons of bridges have been documented arising from heavily corrosion attacks initiated and propagated in the presence of an unhardened (soft) whitish paste generated by segregation. The reasons for this aggressive corrosion attack are not clear, and improving the knowledge on the properties of the segregated grout would help in clarifying this phenomenon. Chemical, physical, and microstructural properties of grouts collected from the ducts of a bridge where segregation occurred are investigated. Results describe the different stages of segregation of the grout and show that the aggressiveness of the whitish grout could be associated with the high content of soluble compounds produced by early hydration of cement, especially alkalis, which lead to pH values exceeding 14. **DOI: 10.1061/(ASCE)MT.1943-5533.0001451.** © *2016 American Society of Civil Engineers.*

Author keywords: Segregation; Grout; pH; Alkalis; Corrosion; Prestressing steel.

Introduction

Prestressing steel, as traditional reinforcing steel, is passive in contact with alkaline cement materials (Bertolini et al. 2013). For this reason, the protection of strands in posttensioned structures can be ensured by the injection in the duct of a cement grout, with appropriate admixtures to increase its stability. The contact with the hardened cement paste provides the chemical conditions required for the passivity of the steel. It is generally assumed that corrosion protection of strands may be guaranteed by the alkalinity of the grout for a long time, unless ducts are not completely filled (i.e., grout lacks in contact with steel), chlorides penetrate through the defects of the duct or the anchors, or hydrogen embrittlement takes place (fib 2005; PTI 2012; Szilard 1969; Schupack 1978; Freyermuth 1991; Schupack 1991; Nagi and Whiting 1996; Henriksen et al. 1998; Nürnberger 2002; Nürnberger and Sawade 2007). Nevertheless, deep corrosion attacks have been recently reported on strands of tendons where segregation of the grout occurred (Godart 2001; Poston and West 2001; Lecinq 2004; Bricker and Shokker 2005; Suarez et al. 2006; Bertolini and Carsana 2006; Powers et al. 2002; Texas Transportation Institute 2009; Carsana and Bertolini 2015). Segregation led to the formation of a whitish unhardened paste (sometimes also called *soft paste*) that was usually found in the highest parts of external posttensioning tendons of box-girder bridges, and it was characterized by an alkaline pH and high content of sulfate ions. Corrosion failure of external tendons can be promoted in a very short period after injection of the grout, e.g., 1–2 years.

The presence of this aggressive paste has been associated to the segregation of the grout injected in the ducts. Several studies have been carried out in order to improve the stability of grouts, thus preventing segregation and related corrosion problems (Poston and West 2001; Chaussin and Chabert 2001; Rosquoe et al. 2003; Schokker et al. 2001; Khayat et al. 1999), and recently specific tests were developed and standardized to assess the stability of the grout [EN 445 (CEN 2005)]. Nevertheless, the aggressive nature of the whitish segregated paste has not been explained yet, and also the reasons why steel wires embedded in this material suffer from fast and heavily penetrating corrosion attacks are still unclear.

This paper describes a study aimed at the characterization of the different types of grout collected on the tendons of a bridge where segregation took place and even the in-service failure of an external posttensioning tendon occurred. Failure happened on one of the 27-strand tendons of a segmental box-girder posttensioned bridge, after less than 2 years from the construction. The ducts were injected with a grout mixed at the construction site with water/cement ratio of 0.32 (w/c) and the addition of a commercial admixture specific for grouts. The fresh grout was able to pass the inclined-tube test and the wick test according to EN 445 standard and thus was considered potentially able to fill the ducts without segregating. Nevertheless, segregation took place due to reasons that could not be assessed, leading to the formation of a whitish unhardened paste [Fig. 1(a)]. Deep localised corrosion attacks were observed on steel in contact with the segregated whitish paste [Fig. 1(b)]. After detection of the failure of one tendon, investigations were carried out on the tendon that failed under service as well as on the other tendons, some of which were replaced, so that a thorough investigation of the grout and the embedded steel strands could be carried out. Results of a detailed inspection, which are described in Carsana and Bertolini (2015), clearly showed that the corrosion attacks only took place on those parts in contact with the segregated grout that was detected in the inclined parts of the tendons between the last deviation points and the anchorages. Therefore, it was decided to better investigate the composition and properties of the grout along the length of ducts. This paper describes a detailed laboratory study carried out on samples of grout collected in different parts of the ducts, aimed at investigating the composition and microstructure of both segregated and nonsegregated grout and

[1]Assistant Professor, Dept. of Chemistry, Materials and Chemical Engineering, "G. Natta" Politecnico di Milano, via Mancinelli, 7, 20131 Milano, Italy (corresponding author). E-mail: maddalena.carsana@polimi.it

[2]Professor, Dept. of Chemistry, Materials and Chemical Engineering, "G. Natta" Politecnico di Milano, via Mancinelli, 7, 20131 Milano, Italy. E-mail: luca.bertolini@polimi.it

Note. This manuscript was submitted on February 14, 2015; approved on August 12, 2015; published online on January 7, 2016. Discussion period open until June 7, 2016; separate discussions must be submitted for individual papers. This paper is part of the ***Journal of Materials in Civil Engineering***, © ASCE, ISSN 0899-1561.

(a) (b)

Fig. 1. Examples of (a) whitish segregated grout in the external posttensioning tendons; (b) severe corrosion attacks on a strand that was in contact with this grout

possible parameters that may influence its aggressiveness toward embedded steel.

Sampling and Laboratory Tests

More than 60 samples representative of different types of grout found along the tendons of the bridge were collected. These were obtained from (1) the tendon that failed in-service, (2) apertures opened in all the tendons of the bridge [Fig. 1(a)], and (3) 10 tendons that were removed and replaced (Carsana and Bertolini 2015). Samples were initially classified according to the consistency and the colour of the grout. This allowed detection of four different types of grout (Fig. 2), which were conventionally identified by the following letters:

- G: Hardened grout with a regular aspect and the typical grey colour;
- B: Hardened grout with a dark grey (almost black) colour;
- W: Unhardened whitish grout (i.e., in the form of a plastic paste, if wet, or a weak and friable material, if dry); and
- P Light grey colored hardened grout with tiny black spots.

Types G and B were found at the bottom of the duct, Type W on the top and Type P at an intermediate position, showing that W and P grouts were the result of segregation of the injected grout. Voids (V) were also found in few cases in the upper part of the duct.

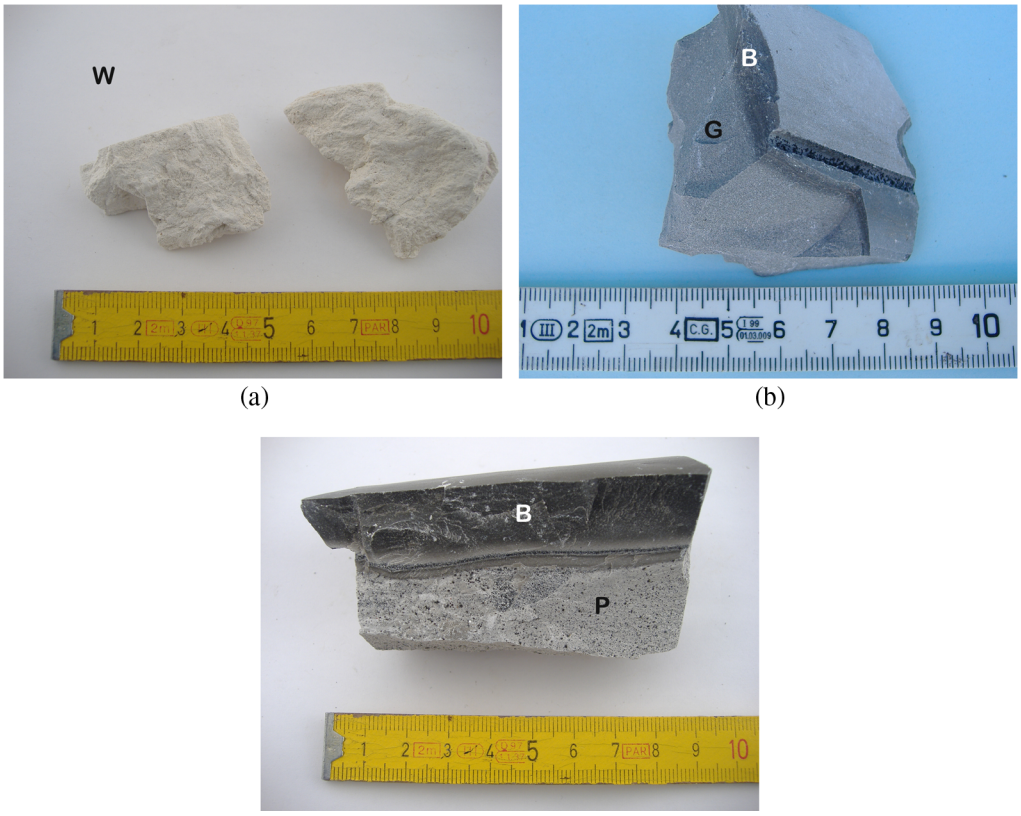

(a) (b)

(c)

Fig. 2. Samples collected from the tendons, showing examples of the different types of grout (W, P, G, and B)

Table 1. Compounds Detected by XRD Analysis and Peaks Intensity (Relative Intensity Is Expressed by the Number of Plus Signs (+), While | Means a Fraction of a Plus Sign and the Dash Means Not Detected)

Type	Sample	Calcite $CaCO_3$	Portlandite $Ca(OH)_2$	Ettringite $Ca_6Al_2(SO_4)_3(OH)_{12} \cdot 26H_2O$	Dolomite ($CaMg(CO_3)_2$ or magnesium oxide (MgO)	Quartz (SiO_2)	Calcium silicate $Ca_2(SiO_4)$	Aphthitalite $K_3Na(SO_4)_2$
W	W1	+++	+	–	–	–	–	|
	W2	++	+++ [a]	–	–	–	–	–
	W3	++ |	+++[a]	–	–	–	–	–
	W4	+++	++[a]	+ |	–	–	–	–
	W5	+++	—	+ |	–	–	–	–
	W6	+++	+++[a]	+ |	–	–	–	–
	W7	+++	++ |[a]	–	–	–	–	–
	W8	+++	—	–	–	–	–	–
P	P1	+++	—	–	|	–	–	–
	P2	+++	+ |[a]	–	–	–	–	–
	P3	+++	—	+	–	–	—	—
G	G1	+++	++ |	+	–	–	—	—
	G2	+++	++	+	–	—	—	—
	G3	+++	++ |	|	–	|	—	—
	G4	+++	++ |	+	–	–	–	–
	G5	+++	+	–	–	–	–	–
	G6	+++	++ |	–	–	–	–	–
	G7	++	+++	–	–	–	–	–
B	B1	+++	++ |	–	–	–	+	–
	B2	+++	++ |	–	|	|	+	–
	B3	+++	++ |	–	—	|	+	–

[a]An anomalous peak of high intensity was observed in the diffractogram, probably due to orientation of portlandite crystals in W grouts and occasionally in P grouts.

Penetrating corrosion attack were observed only on steel wires in contact with the W grout (corrosion rate of several mm/year could be estimated), whilst shallow and small corrosion spots were occasionally observed on steel embedded in type P grout; no corrosion was found on the major portions of the strands embedded in G and B grouts (Carsana and Bertolini 2015).

In order to investigate on the composition, microstructure, and thus the aggressiveness of the different types of grout towards embedded steel, laboratory analyses were carried out on selected samples. X-ray diffraction (XRD) analyses were carried out on powders using a diffractometer with CuKα radiation and a scan rate of 2.4° min^{-1}. The identification of crystalline compounds was performed by the software *Philips X'Pert SW* and then verified manually with the joint committee on powder diffraction standards (JCPDS) database. From the peaks present in the diffraction patterns, the compounds reported in Table 1 were detected. A qualitative description of the relative intensity of the peaks is also shown in Table 1 by the number of plus (+) symbols. Thermogravimetric analyses (TGA) and differential thermal analysis (DTA) were also carried out. From the TGA curve, mass losses were identified in some significant intervals of temperature, which are summarized in Table 2. Samples were initially heated at 70°C to allow evaporation of free water. In the range of 70–390°C, the loss of water adsorbed and bound in the hydration products was detected. This loss continued in the range 390–550°C and in some samples the DTA analysis showed an endothermic peak in the range 390–450°C, which can be traced to the loss of water resulting from the dehydration of the calcium hydroxide ($Ca(OH)_2 \rightarrow CaO + H_2O$). In these cases, the sum of the mass losses in the two subintervals of 390–450 and 450–550°C are reported in Table 2. The loss of mass in the range 550–750°C is attributed to the presence of calcium carbonate which decomposes, releasing carbon dioxide ($CaCO_3 \rightarrow CaO + CO_2$), and leads to an endothermic peak in the DTA curve.

The elemental composition of the grout was analysed by plasma inductively coupled plasma optical emission spectrometry (ICP-OES) and it was expressed in terms of oxides, as shown in Table 3.

Table 2. Mass Loss (%) Detected at Specific Temperature Ranges during TGA–DTA Analyses

Grout type	Sample	70–390°C	390–550°C[a]	550–750°C
W	W1	4.1	6.07	21.39
	W2	6.16	3.82 + 1.99	17.71
	W3	7.25	2.78 + 1.57	14.22
	W7	7.1	2.24 + 1.67	15.79
	W8	7.71	6.07	13.75
	W9	5.81	2.94 + 2.81	20.7
P	P1	8.42	3.6	11.74
	P2	7.5	2.41 + 0.86	13.99
	P3	6.61	3.85	8.47
G	G3	5.94	3.75 + 0.8	5.91
	G4	7.27	4.21 + 0.79	7.68
	G5	9.35	2.29 + 0.99	14.04
	G6	8.36	4.15 + 0.76	8.98
	G7	8.51	4.56 + 0.75	7.86
	G8	10.23	3.66 + 0.77	9.26
B	B1	7.26	3.62 + 0.66	8.28
	B2	7.79	3.77 + 0.75	7.10
	B3	6.85	3.51 + 0.69	6.94

[a]For those samples that showed a DTA peak corresponding to the presence of calcium hydroxide, in this range of temperature, the two mass losses measured in the intervals 390–450°C (corresponding to loss of water in calcium hydroxide) and 450–550°C have been indicated separately.

The content of sulphates and insoluble residue were also measured with traditional chemical analysis of the samples dissolved in hydrochloric acid. The results are summarized in Table 4. Several samples were also subjected to analysis of the chloride content, but no appreciable amounts of these ions were detected.

The density of the grout was measured on small fragments (a few cm^3), both in dry and water-saturated conditions. The volume of the samples was estimated using a pycnometer. From the variation of mass between the dry and the water-saturated samples, the water absorption was also calculated. The results are shown in

Table 3. Results of Elemental Chemical Composition Measured by Means of ICP-OES Analysis, Expressed as % Oxide versus Dry Mass

Grout type	Sample	Al_2O_3	CaO	K_2O	Na_2O	MgO	Fe_2O_3	SO_3	SiO_2
W	W1	1.18	32.34	4.00	2.40	0.88	1.02	6.95	2.63
	W2	1.68	47.04	1.55	0.96	1.35	1.26	7.88	7.91
	W3	2.02	40.32	1.30	0.78	1.40	1.27	6.73	10.30
	W7	1.78	40.60	0.66	0.47	1.48	1.49	3.58	8.13
	W8	1.79	38.64	1.40	1.24	1.18	1.93	7.50	11.76
	W9	1.34	38.36	0.70	0.66	1.10	1.17	6.68	2.05
	Average	1.62	38.05	1.61	1.11	1.21	1.38	6.29	6.97
P	P1	1.49	36.06	1.02	0.69	1.63	1.34	2.45	11.46
	P2	2.04	47.32	1.19	0.73	1.53	1.69	4.90	12.19
	P3	1.23	25.06	1.17	0.66	1.00	1.14	2.00	5.26
	Average	1.57	36.15	1.13	0.69	1.39	1.39	3.12	9.64
G	G3	1.69	46.69	0.35	0.32	1.95	1.13	1.75	2.44
	G4	2.40	43.26	0.49	0.39	1.72	2.07	2.50	11.31
	G5[a]	1.61	39.62	0.99	0.63	1.28	1.39	4.15	12.83
	G6	2.42	45.78	0.58	0.42	1.75	2.06	2.83	12.75
	G7	2.47	47.18	0.57	0.49	1.92	2.27	2.63	13.05
	G8	2.23	43.4	0.29	0.27	1.65	2.00	2.08	11.34
	Average	2.14	44.32	0.55	0.42	1.71	1.82	2.66	10.62
B	B1	2.08	48.02	0.34	0.30	1.83	1.07	1.93	9.28
	B2	2.80	49.28	0.34	0.34	2.78	2.47	1.98	11.34
	B3	1.13	40.04	0.37	0.31	1.37	0.44	1.65	4.49
	Average	2.00	45.78	0.35	0.32	1.99	1.33	1.85	8.37

[a]This sample was in contact with *P* grout.

Table 4. Insoluble Residue and Sulphate Ion Content (% by Mass)

Grout type	Sample	Insoluble residue	Sulphates (% SO_3)
W	W1	0.30	6.26
	W3	1.88	5.67
	W7	4.31	3.57
	W8	0.02	6.15
	W9	—	6.62
	Average	1.63	5.65
P	P1	6.26	3.50
	P2	1.76	5.08
	P3	10.07	3.99
	Average	6.03	4.19
G	G3	9.99	1.54
	G4	0.53	2.48
	G5[a]	—	4.32
	G6	1.30	2.57
	G7	—	2.20
	G8	—	2.73
	G9	—	1.91
	Average	3.94	2.53
B	B1	10.29	2.04
	B2	1.56	2.25
	B3	4.09	1.62
	Average	5.31	1.97

[a]This sample was in contact with P grout.

Table 5. Finally, the microstructure of the samples of grout was observed under a stereomicroscope and an environmental scanning electron microscope with an X-ray energy dispersive spectrometer (EDS). Figs. 3–6 show examples of the typical microstructures and EDS spectra of the different types of grout.

Discussion

Composition, microstructure, and other properties of grout samples will be first analyzed for each type of grout. Then an attempt to identify features that may lead to lack of steel protection is made.

Table 5. Density in Water-Saturated and Dry Conditions and Water Absorption

Grout type	Sample	Saturated density (kg/m^3)	Dry density (kg/m^3)	Water absorption (% by mass)
W	W7	1,501	791	89.7
	W10	1,365	547	149.8
	Average	1,433	669	119.8
P	P1	1,733	1,292	34.1
	P2	1,576	903	74.5
	P4	1,599	893	79.1
	P5	1,648	1,021	61.3
	Average	1,639	1,027	62.2
G	G3	2,049	1,660	23.4
	G5	1,841	1,293	42.4
	G10	2,105	1,716	22.7
	G11	2,041	1,668	22.4
	G12	1,926	1,513	27.2
	G13	2,247	1,914	17.4
	G14	1,897	1,506	25.9
	G15	2,092	1,685	24.1
	G16	1,952	1,522	28.2
	G17	2,116	1,707	23.9
	G18	2,066	1,678	23.1
	G19	2,041	1,641	24.4
	G20	2,151	1,725	24.7
	G21	2,057	1,668	23.3
	G22	2,070	1,601	29.3
	Average	2,042	1,635	25.5
B	B1	2,273	1,991	14.2
	B2	2,223	1,928	15.3
	B3	2,134	1,803	18.3
	B4	2,186	1,900	15.0
	B5	2,218	1,910	16.1
	B6	2,304	2,000	15.2
	Average	2,223	1,922	15.7

Grout G

The microstructure of Grout G [Fig. 2(b)], observed with the scanning electron microscope, shows the typical aspect of a hardened cement paste [Fig. 3(a)] and the presence of chemical elements typical of calcium silicate and aluminate hydrates [Fig. 3(b)]. XRD analysis (Table 1) detected the presence of calcite ($CaCO_3$), portlandite ($Ca(OH)_2$), and, to a lesser extent, ettringite ($Ca_6Al_2(SO_4)_3(OH)_{12} \cdot 26H_2O$). Thermal analyses confirmed the presence of calcium hydroxide, shown in the range 390–450°C by an endothermic peak in the DTA curves and a mass loss of about 4% in the TGA curves (Table 2). Oxide content estimated from ICP-OES analysis showed expected values for a hardened cement grout (Table 3); in particular, the average values of the contents of alkalis are 0.55 and 0.42%, respectively, for potassium oxide (K_2O) and sodium oxide (Na_2O). Also, the sulphate content is in the expected range (expressed as SO_3, average values of 2.66 and 2.53% were obtained, respectively, by ICP-OES and traditional chemical analyses, Tables 3 and 4). Only Sample G5 showed higher values both of alkalis and sulphates. Since this sample of Grout G was in contact with Grout P, is it reasonable to assume that there has been a contamination and the results are not representative of Grout G; values for this sample, however, have been considered in the calculation of average values.

The average density measured on the samples of Grout G is 2,042 kg/m^3 in the water-saturated condition and 1,635 kg/m^3

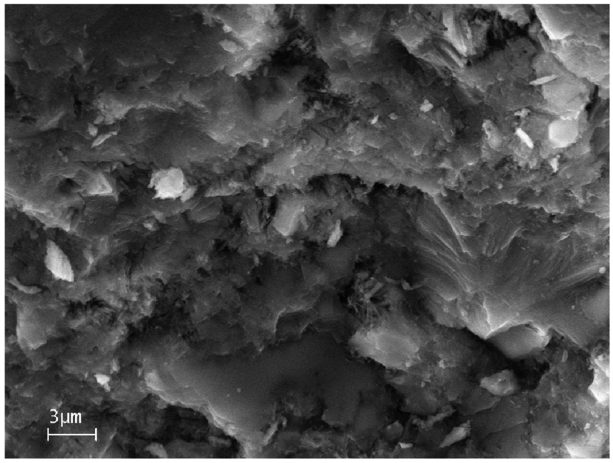

(a)

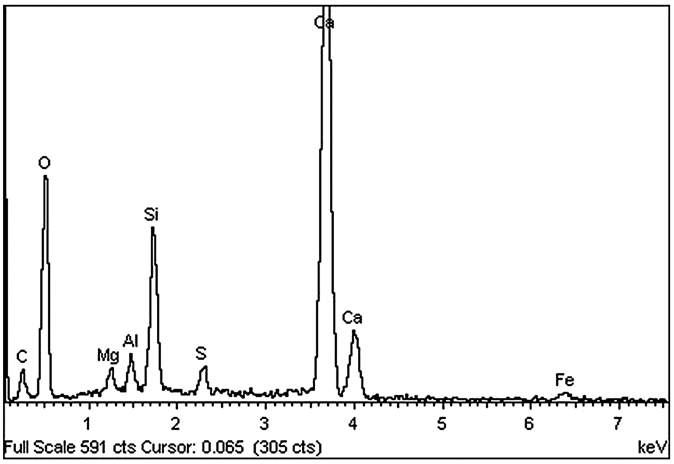

(b)

Fig. 3. (a) SEM image; (b) EDS analysis Grout G (Sample G8)

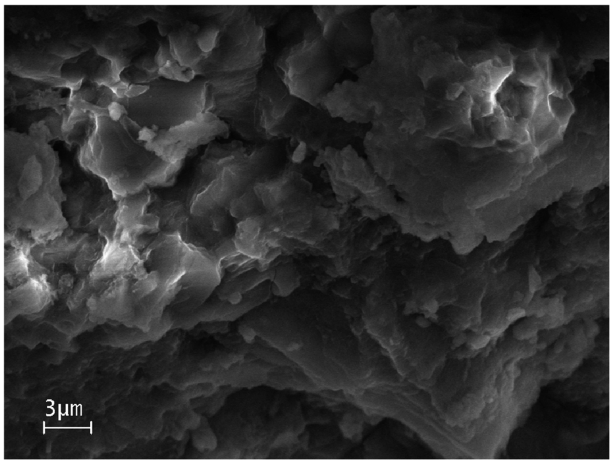

(a)

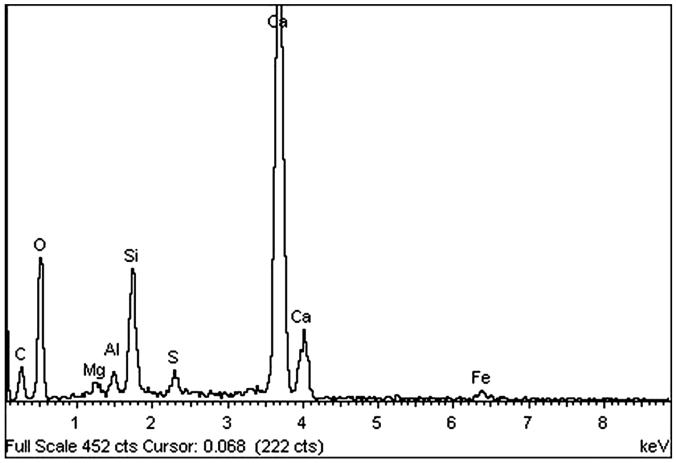

(b)

Fig. 4. (a) SEM image; (b) EDS analysis of Grout B (Sample B1)

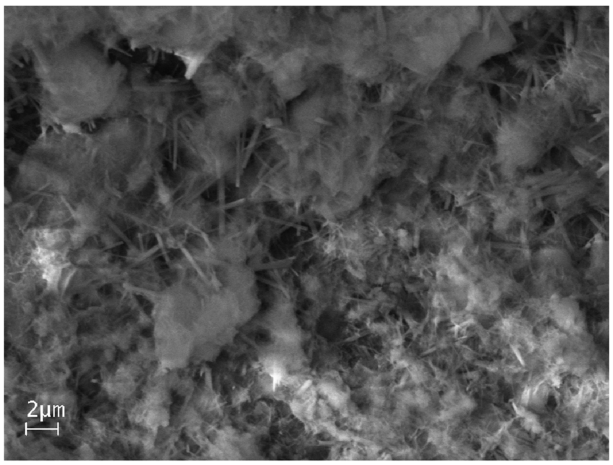

(a)

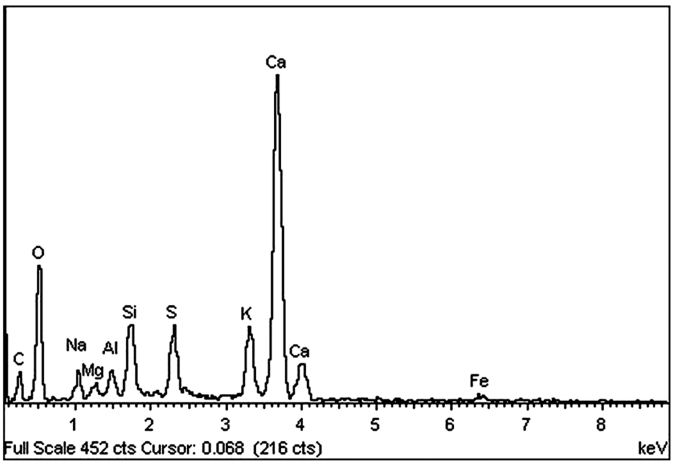

(b)

Fig. 5. (a) SEM image; (b) EDS analysis of Grout W (Sample W3)

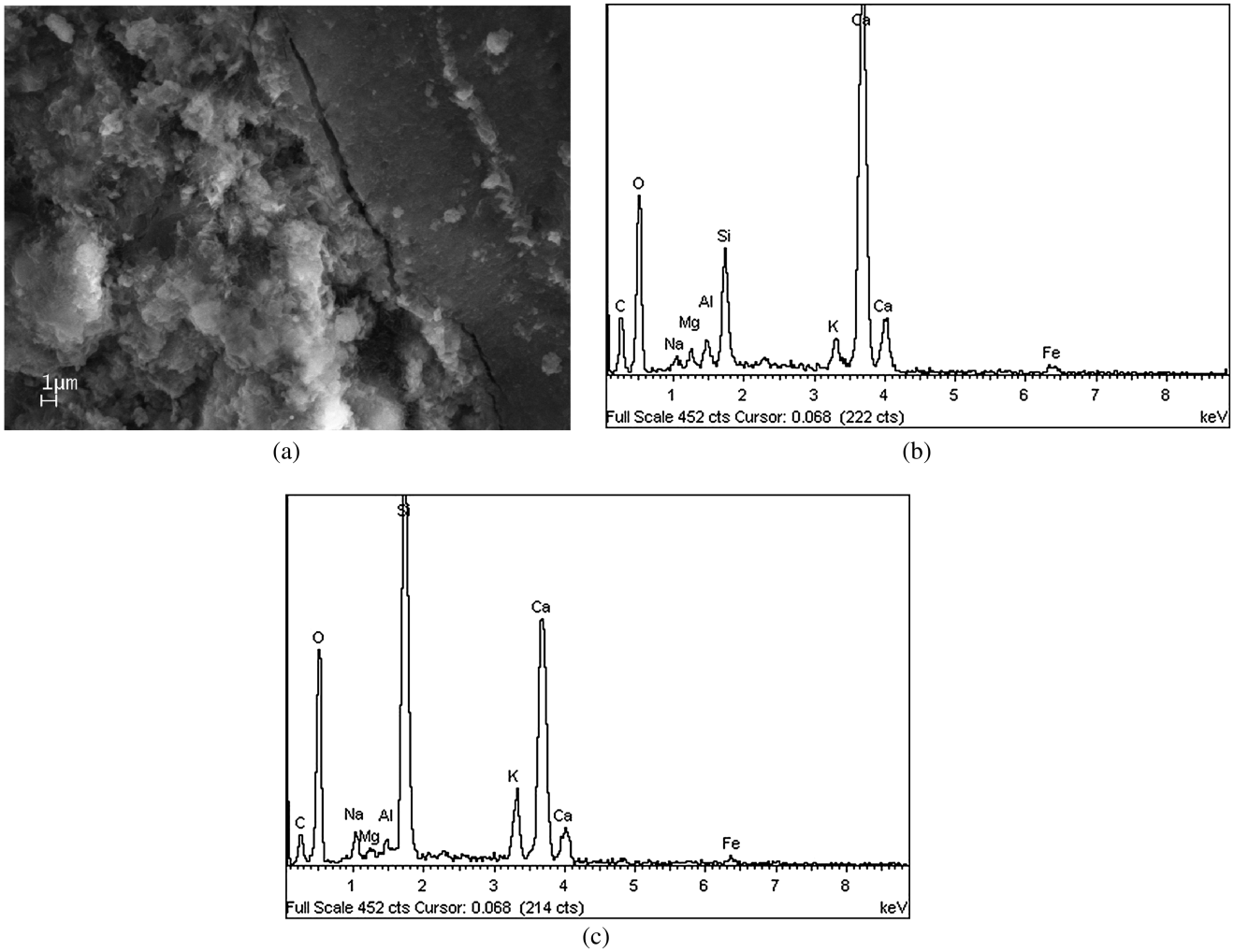

Fig. 6. (a) SEM image of Grout P (Sample P1) and EDS analysis of the cement matrix on the (b) left and (c) the dark spot on the right

in the dry condition; water absorption is 25.5% on average (Table 5). Similar results were also obtained from measurements on removed tendons on which the inspection was carried out for the entire length of the tendon [as described in Carsana and Bertolini (2015)]. The values of density of the saturated material are compatible with the nominal water/cement ratio of the grout. This is shown in Fig. 7 where a theoretical relationship between water/cement ratio and the density of the fresh grout (calculated assuming a density of 1 kg/L for water and 3.10 kg/L for cement, and neglecting for the admixture) is reported, showing that the average water-saturated density of 2,040 kg/m^3 for G grouts fits with a water/cement ratio of about 0.32. This means that the Grout G, which was found to fill most of the volume of the ducts, was as expected from the nominal composition of the injected grout.

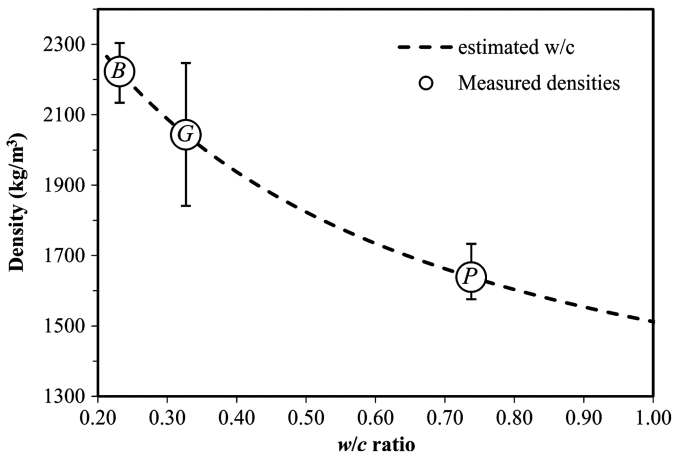

Fig. 7. Theoretical relationship between the fresh density of grout and w/c ratio, compared with the measured density of the water-saturated grouts (average value, circle, and range of variation)

Grout B

Samples of Grout B [Fig. 2(c)] at a microscopic level showed a compact structure [Fig. 4(a)]. Compared to samples of Grout G, they have higher density (average value of 2,223 kg/m^3 in saturated condition) and lower water absorption (15.7% by mass, Table 5). The results of EDS [Fig. 4(b)], XRD (Table 1), and thermal (Table 2) analyses are similar to those of samples of Grout G. ICP-OES analysis shows a slightly lower content of soluble compounds: the average values of the alkalis are respectively 0.35 and 0.32% by mass for Na_2O and K_2O, while the mean value of sulphate (expressed as SO_3) is 1.85% (1.97% from traditional chemical analysis, Table 4). This shows that the Grout B, while presenting the typical characteristics of hardened cement paste,

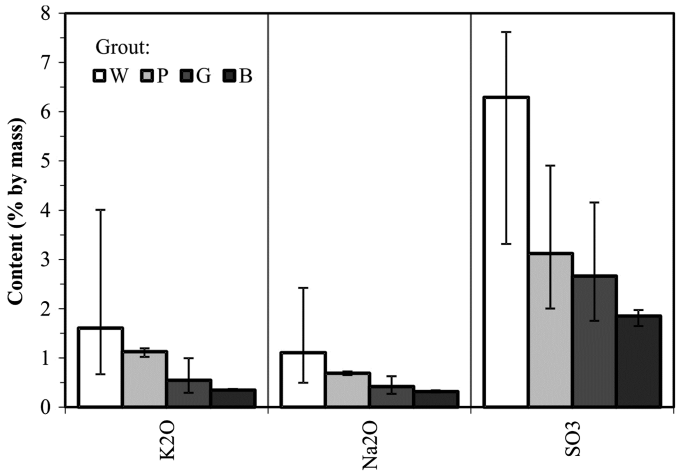

Fig. 8. Comparison of alkalis and sulphate ions content in the different types of grout

has a greater compactness than Grout G. The fact that this type of grout has been identified mainly in the lower part of the ducts suggests that it was produced as the consequence of sedimentation of the fresh grout during the injection or in the moments immediately following, with local reduction of the content of water and the consequent formation of a hydrated cement paste with a lower w/c ratio (Fig. 7), therefore, lower porosity.

Grout W

The grout of type W was found in the higher parts of the tendons (especially in the side opposite to that where the grout was injected) and it was observed in various forms (Carsana and Bertolini 2015). When it was observed immediately following the apertures of the ducts, it usually had a plastic consistence, while after drying it appeared as friable and brittle. Fig. 5 shows that at SEM observation, the microstructure is very porous and shows only few crystals that interconnect different particles and give some cohesion to the sample [Fig. 5(a)]. Chemical elements typical of the hydration products of cement hydration were detected by EDS analyses, but compared to G and B grouts, peaks of alkalis (Na and K) and sulphur (S) are more pronounced, Fig. 5(b).

XRD analysis (Table 1) showed the presence of calcite, portlandite, and ettringite, while thermal analyses (Table 2) showed a lower mass loss associated to calcium hydroxide compared to Grouts B and G, and the endothermic peak of this compound was even not visible in the DTA curve of some samples. Chemical analyses showed very high and variable values for soluble compounds (Table 3). Alkalis had average values of 1.61 and 1.11% for K_2O and Na_2O, but even reached respective values of 4.0 and 2.4% (Fig. 8). Sulphates showed an average value of 6.29%, and a maximum value of 7.88% (Tables 3 and 4). For this grout, the estimation of the density was difficult because the material is soluble in water. The analyses carried out on two samples that showed a higher consistency (Table 5), confirmed the high porosity of the material, characterized by values of water absorption close to or above 100% and mean water-saturated density of only 1,433 kg/m^3.

From the results outlined in the preceding paragraphs, it can be observed that this material has a high concentration of the chemical elements that are in a solution in the early stages of hydration of the cement paste, in particular sulphates, due to the presence of gypsum as a set regulator, and alkalis, released by early hydration of clinker. Accumulation in the higher areas of the ducts of bleeding water and more-soluble compounds has therefore led to the formation of the W type grout. Since immediately after the aperture of the ducts, this material appeared soaked by water even after more than 2 years after the injection, it can be considered that the wet whitish grout remained in contact with the strands for a long period.

The high amount of alkalis detected in the samples analyzed indicates that the moist Grout W had an extremely high concentration of hydroxyl ions (OH^-). In fact, the high solubility of Na_2O and K_2O leads to a concentrated NaOH and KOH solution, which impregnates grout. The lower content of $Ca(OH)_2$ found in these samples is compatible with the high alkali content; in fact, the solubility of calcium hydroxide decreases by increasing concentration of alkalis, which promote its precipitation in the form of portlandite crystals. To estimate the pH of the liquid phase of the wet whitish grout, pH measurements were carried out both with colour pH indicators and direct measurements with a glass electrode on solutions extracted from the grout. However, it was only possible to assess the high pH of this solution, but no reliable values could be measured since pH measurement methods are not effective when values are close or higher than 14. To estimate indirectly the pH of this solution, Sample W7 (characterized by 0.66% K_2O and 0.47% Na_2O, referred to the dry mass of the sample) was considered and the amount of water needed to bring the sample to a plastic consistence similar to that observed in the duct just open was calculated. Assuming that the alkali present in the sample is completely dissolved in that quantity of water to form KOH and NaOH, the concentration of OH^- ions and, therefore, the pH of the solution were calculated around a value of 14.3. This calculation, although approximate and simplified, shows how the white wet grout can be characterized by extremely high values of pH.

Grout P

The P type of grout was found in the intermediate position between Grouts G or B and Grout W. To the naked eye, this grout shows a cement matrix of grey colour lighter than that of Grout G and uniformly distributed dark spots with size of the order of 0.1 mm [Fig. 2(c)]. At the scanning electron microscope, the grey matrix [left part in Fig. 6(a)] has the typical morphology of a hardened cement paste. The right part of Fig. 6(a) shows one of the particles that constitute the dark spots visible to the naked eye. The microstructure of these particles is very compact and EDS analysis [Fig. 6(c)] shows a very high peak of silicon.

XRD (Table 1) and thermal (Table 2) analyses provided for Grout P results similar to those obtained for Grout W. ICP-OES analysis carried out on three samples (Table 3), provided highly variable results, especially with regard to the estimated content of oxides that can be traced back to the products of hydration of calcium silicates (CaO and SiO_2, but also MgO). However, high values of alkalis (1.13 and 0.69%, respectively for K_2O and Na_2O on average, Fig. 8) and sulphates (average value of 3.12%) were found. Also the samples analyzed with traditional chemical analysis (Table 4) gave high values of sulphate content (4.19%) and showed a great variability between samples. Average density (Table 5) was 1,639 kg/m^3 for the saturated material and 1,027 kg/m^3 for the dry material, while absorption was 62% by mass. Assuming valid the relationship shown in Fig. 7, a water/cement ratio much higher than the nominal value can be estimated for this grout.

Summarizing the previous observations, Grout P can be regarded as an intermediate stage of segregation compared to Grout W. In fact, it is reasonable to assume that segregation that occurred prior to the setting of the grout determined a local increase

in the water content and, therefore, in the water/cement ratio. This did not prevent, as occurred in the case of Grout W, the formation of aluminates and calcium silicate hydrates and, therefore, the setting and hardening of Grout P. However, the increase of the w/c ratio led to a more-porous microstructure. Furthermore, the water that concentrated in these areas, similarly as in Grout W, resulted in a high concentration of most soluble hydration products (alkalis and sulphates).

It may be considered that the transition from Grout P to Grout W represents different stages of segregation in which the amount of segregated water, as well as ions dissolved in it, increase and the material progressively loses strength due to the increase in porosity and the impossibility to form a sufficiently dense network of hydration products.

Aggressiveness of W and P Grouts

Grout W was found to be aggressive towards embedded steel strands. Heavily localized corrosion attacks, as shown for example in Fig. 1(b), took place with an extremely high corrosion rate (several mm/year). Results of the tests described in this paper clearly showed that the whitish grout produced by segregation is highly alkaline and does not contain chloride ions. Therefore, corrosion cannot be ascribed to carbonation, because of the alkaline nature of the segregated grout as well as the extremely localized morphology of the corrosion attacks (furthermore, carbonation is hindered inside the plastic ducts since penetration of carbon dioxide is prevented). On the other hand, the absence of appreciable amounts of chloride ions in the grout does not allow that pitting corrosion could take place. No sign of stress corrosion cracking was observed on the corroded strands, and even the presence of stray current inside the plastic ducts has to be definitely excluded (Carsana and Bertolini 2015). As a matter of facts, the usual causes of steel corrosion in concrete (Bertolini et al. 2013; Tuutti 1982; Bertolini 2008) cannot be responsible of the corrosion attacks observed in the posttensioning strands of the bridge.

By comparing the composition of Grout W with that of Grouts G and B, which was shown to clearly allow the expected passivation of steel (Carsana and Bertolini 2006), it can be observed from the results described in this paper that the aggressiveness of the former can only to be traced back to the high pH, and the high concentration of alkalis or sulphate ions. This conclusion, however, requires an explanation for the electrochemical mechanism through which a grout with such properties may be highly aggressive for steel strands. Bertolini and Carsana (2006), on the basis of preliminary corrosion tests, made an attempt to propose a mechanism for this type of corrosion, suggesting that, in the highly alkaline environment generated by the wet W grout, conditions of low availability of oxygen may be produced in the interstices among wires of the strands, which can be responsible for the corrosion initiation, while the subsequent high rate of propagation of the attack can be ascribed to the macrocells that generates in the highly electrically conductive whitish paste between the small depassivated areas and the surrounding passive areas of the steel. Further investigations are being carried out in order to confirm this corrosion mechanism.

Grout P, being an intermediate state of segregation between the ordinary Grout G and the unhardened Grout W, was essentially protective towards steel, since most of the steel in contact with this material was found to be passive. Nevertheless, some small rust spots could be found in some cases (Carsana and Bertolini 2015), showing that, even though Grout P was able to harden, in some cases, probably associated with local concentration of alkalis, conditions able to allow steel depassivation could be promoted.

Conclusions

The different types of grout found along the length of tendons of a bridge were attributed to segregation that occurred inside the ducts, leading to the formation of an aggressive whitish unhardened paste in small portions of the tendons in the vicinity of the anchorages. Most of the grout along the duct was a common hardened cement paste of grey colour (Grout G), which had composition, microstructure, and properties compatible with those expected according to the nominal composition of the grout that was injected in the ducts. This grout allowed full passivation of the steel.

In those portions of the tendons where segregation took place, other types of grout were found. A darker grout (Grout B) was occasionally found at the bottom of the duct, which was found to be a denser hydrated cement paste with lower w/c ratio, but still allowed passivation of the steel. Conversely, in the upper part of the ducts, an unhardened whitish paste was found, which was extremely aggressive for the embedded steel strands. This grout was found to be enriched in the most soluble compounds produced by early hydration of portland cement, i.e., alkalis, sulphate, and hydroxyl ions, which could justify that pH values even exceeding 14 were estimated. The initiation and propagation of deep localized corrosion attacks on steel embedded in this segregated grout have to be related to these features, as the chloride content was negligible. An intermediate stage of segregation was also found between Grouts W and G, consisting in a hardened cement paste of light grey colour showing small dark spots to the naked eye (Grout P). Although this grout, which had a lower density and a higher concentration of soluble ions compared to the ordinary Grout G, was able to promote protect steel in most cases, but was not able to fully passivate the steel strands.

References

Bertolini, L. (2008). "Steel corrosion and service life of reinforced concrete structures." *Structure Infrastr. Eng: Maint, Management, Life-Cycle Des. Perform.*,4(2), 123–137.

Bertolini, L., and Carsana, M. (2006). "High pH corrosion of prestressing steel in segregated grout." *Modell. Corroding Concr. Struct.*, C. Andrade and M. Mancini, eds, Rilem, Springer, Netherlands, 147–158.

Bertolini, L., Elsener, B., Pedeferri, P., Redaelli, E., and Polder, R. (2013). *Corrosion of steel in concrete—Prevention, diagnosis, repair*, 2nd Ed., Wiley-WCH, Weinheim, Germany.

Bricker, M. D, and Shokker, A. J. (2005). "Corrosion from bleed water in grouted post-tensioned tendons." Portland Cement Association, Skokie, IL.

Carsana, M., and Bertolini, L. (2015). "Corrosion failure of post-tensioning tendons in alkaline and chloride-free segregated grout: A case study." *Struct. Infrastruct. Eng.*, 11(3), 402–411.

CEN (European Committee for Standardization). (2005). "Grout for prestressing tendons—Test methods." *EN 445*, Brussels, Belgium.

Chaussin, R. (2001). "Strategies for improvement—Approach in France." International Federation for Structural Concrete (fib), Lausanne, Switzerland, 235–244.

fib (International Federation for Structural Concrete). (2005). "Durability of post-tensioning tendons." *fib Bulletin No. 33*, Lausanne, Switzerland.

Freyermuth, C. L. (1991). "Durability of post-tensioned prestressed concrete structures—An overview of research and experience." *Concr. Int.*, 13(10), 58–65.

Godart, B. (2001). "Status of durability of post-tensioned tendons in France." International Federation for Structural Concrete (fib), Lausanne, Switzerland, 25–42.

Henriksen, C. F., Knudsen, A., and Braestrup, M. W. (1998). "Cable corrosion: Indetected." *Concr. Int.*, 20(10), 59–72.

Khayat, K. H., Yahina, A., and Duffy, P. (1999). "High-performance cement grout for post-tensioning applications." *ACI Mater. J.*, 96(4), 471–477.

Lecinq, B. (2004). "Recent research in France for the improvement of cement grouting." *Proc., 2nd Workshop on Durability of Post-Tensioning Tendons*, ETH, Zürich, Switzerland.

Nagi, N., and Whiting, D. (1996). "Corrosion of prestressed reinforcing steel in concrete bridges: State-of-the-art." American Concrete Institute, Farmington Hills, MI.

Nürnberger, U. (2002). "Corrosion induced failure mechanism of prestressing steel." *Mater. Corros.*, 53(8), 591–601.

Nürnberger, U., and Sawade, G. (2007). "Degradation of prestressed steel." *Durability of concrete and cement composites*, C. L. Page and M. M. Page, eds., Woodhead, Cambridge, U.K., 187–246.

Poston, R. W., and West, J. S. (2001). "North American strategies for improving bonded post-tensioned concrete construction." International Federation for Structural Concrete (fib), Lausanne, Switzerland, 245–255.

Powers, R. G., Sagues, A. A., and Virmani, Y. P. (2002). "Corrosion of post-tensioned tendons in Florida bridges." ⟨http://www.dot.state.fl.us⟩ (Jan. 15, 2015).

PTI (Post-Tensioning Institute). (2012). "Specification for grouting of post-tensioned structures." *PTI M55.1-12*, Farmington Hills, MI.

Rosquoe, F., Alexis, A., Khelidj, A., and Phelipot, A. (2003). "Experimental study of cement grout: Rheological behavior and sedimentation." *Cem. Concr. Res.*, 33(5), 713–722.

Schokker, A. J., Breen, J. E., and Kreger, M. E. (2001). "Grouts for bonded post-tensioning in corrosive environments." *ACI Mater. J.*, 98(3), 296–305.

Schupack, M. (1978). "A survey on the durability performance of post-tensioning tendons." *ACI J.*, 75(10), 501–510.

Schupack, M. (1991). "Corrosion protecion for unbonded tendons." *Concr. Int.*, 13(2), 51–57.

Suarez, J., Zhang, J., Hsuan, G., and Hartt, W. (2006). "Polyethylene duct cracking on post-tensioning tendons in Florida segmented bridges." *J. Mater. Civ. Eng.*, 10.1061/(ASCE)0899-1561(2006)18:4(581), 581–587.

Szilard, R. (1969). "Corrosion and corrosion protection of tendons in prestressed concrete bridges." *ACI J.*, 66(1), 42–59.

Texas Transportation Institute. (2009). "Effect of voids in grouted, post-tensioned concrete bridge construction." ⟨http://tti.tamu.edu/documents/0-4588-1-Vol1.pdf⟩ (Jan. 15, 2015).

Tuutti, K. (1982). "Corrosion of steel in concrete." Swedish Foundation for Concrete Research, Stockholm, Sweden.